Effect of Additives, Catalyst Residues, and Confining Substrates on the Fractionated Crystallization of Polypropylene Droplets

Deepak S. Langhe, Anne Hiltner, Eric Baer

Department of Macromolecular Science and Engineering, Case Western Reserve University, Cleveland, Ohio

Received 25 August 2011; accepted 3 October 2011
DOI 10.1002/app.36300
Published online 20 January 2012 in Wiley Online Library (wileyonlinelibrary.com).

ABSTRACT: Fractionated crystallization of Ziegler-Natta PP (ZN-PP) droplets produced from ZN-PP/polystyrene (PS) multilayered films resulted in four crystallization exotherms at 40, 64, 90, and 103°C. The origins of these crystallization peaks were investigated in this article. The nucleation of ZN-PP droplets at various crystallization exotherms was attributed to (1) various additives in ZN-PP and PS, (2) catalyst residues present in ZN-PP, or (3) substrate nucleation by confining matrix. Effect of various additives on the fractionated crystallization an additive-free grade of ZN-PP (cPP) was investigated. Crystallization of cPP droplets from 200-nm layers showed that Irganox was responsible for crystallization of droplets at 103°C. Irgafos and ZnS did not affect the crystallization of cPP droplets. We also investigated three grades of PP, which were synthesized using different catalysts. The PP grades were ZN-PP, developmental PP (D-PP) and metallocene PP (M-PP). D-PP droplets from 200-nm layers showed crystallization at 100°C, while ZN-PP resulted in crystallization at 90 and 103°C. It was suggested that the 90°C peak for ZN-PP droplets was most likely due to the presence of Ziegler-Natta catalyst residues. Crystallization of M-PP droplets produced from 200 nm showed multiple crystallization exotherms (60 to 90°C). The effect of confining substrates on the fractionated crystallization of ZN-PP droplets revealed heterogeneous nucleation by polycarbonate (PC) substrate. When the confining matrix was changed from polystyrene (PS) to polymethyl methacrylate (PMMA), the crystallization thermograms of ZN-PP droplets were unaffected. © 2012 Wiley Periodicals, Inc. J Appl Polym Sci 125: 2110–2120, 2012

Key words: polypropylene; fractionated crystallization; additives; heterogeneous nucleation

INTRODUCTION

Crystalline polymers exhibit multiple crystallization exotherms when dispersed in small domains. This phenomenon is known as fractionated crystallization.[1,2] The crystallization behavior of dispersed polymer systems is drastically different from the bulk crystallization of polymers. Crystallization of polymers in the bulk usually initiates at heterogeneous nuclei, such as additives, catalyst residues, high molecular weight gel particles, or dust particles. Fractionated crystallization results from the separation of these active heterogeneities in individual crystallizable domains. Activation of nuclei at different temperatures results in multiple crystallization exotherms of the polymer domains. Each crystallization exotherm is attributed to the crystallization of a number of domains by a specific type of nuclei. Fractionated crystallization separates the nuclei that would otherwise not be observed during crystallization of bulk polymer.

Various approaches have been used to create the domains or droplets of crystallizable polymers to investigate the fractionated crystallization.[3–10] Dispersions of crystalline polymer droplets in an amorphous matrix were obtained by conventional blending techniques.[4,5]Controlling droplet size distribution is one of the limitations of this method. Block copolymers have also been synthesized to control the size of crystallizing domains.[6–8] However, custom synthesis of copolymers with at least one crystallizable block limits the choices of polymers that can be used in this technique. An approach involving dewetting of spin coated ultrathin films was also employed to produce droplets for visualization of the crystallization process.[9] Only a few polymers can be investigated using this approach. Another solvent based technique involved the spraying of polymer solutions to produce droplets.[10]

A novel approach of interfacially driven thermal break up of multilayered films result in a dispersion of polymer droplets into an amorphous polymer matrix. Droplets of high density polyethylene (HDPE)

Correspondence to: D. S. Langhe (deepak@case.edu).
Contract grant sponsor: NSF Science and Technology Center for Layered Polymeric Systems; contract grant number: 0423914.

TABLE I
Different Additives Present in ZN-PP and PS

Polymer	Additive	Category	Concentration (ppm)
Ziegler-Natta Polypropylene (ZN-PP)	Irganox 1010	Primary antioxidant	10^3
	Irgafos 168	Secondary antioxidant	10^3
	Synthetic hydrotalcite	Neutralizer	300–500
	Catalyst residues	Catalyst	–
Polystyrene (PS)	Zinc stearate	Mold release agent	–

Information obtained from The Dow Chemical Company.

or polypropylene (PP), dispersed in a polystyrene (PS) matrix, were successfully produced using this nonsolvent technique.[11–13] The flexibility of the forced assembly coextrusion process enabled the control of droplet size distribution by changing the starting layer thickness. It is interesting to note that this technique does not utilize any compatibilizer to produce dispersion of droplets, and the approach can be extended to a wide variety of melt processible polymers.

In the fractionated crystallization thermograms, the lowest temperature exotherm is due to homogeneous nucleation, while the higher temperature exotherms are due to heterogeneous nucleation of droplets. The specific nuclei activated in higher temperature crystallization exotherms are still not known. The goal of this paper is to identify the heterogeneous nuclei responsible for fractionated crystallization of PP droplets. Previously, the crystallization of Ziegler-Natta polypropylene (ZN-PP) droplets, produced from multilayered films, showed four crystallization exotherms at 40, 64, 90 and 103°C. The lowest temperature exotherm at 40°C resulted from homogeneous nucleation. Origins of the other three crystallization peaks were attributed to either (1) various additives from ZN-PP or the confining matrix, (2) catalyst residues present in ZN-PP, or (3) substrate nucleation by the confining matrix. Two major additives—Irganox and Irgafos—were identified to be present in ZN-PP. These additives were blended with an additive-free grade of ZN-PP (cPP) at different concentrations and coextruded with PS by the multilayer film extrusion process. The effect of additive concentration on crystallization enthalpies was investigated. Another additive present in PS, zinc stearate (ZnS), was also studied. To probe the possibility of nucleation by catalyst residues, fractionated crystallization of three grades of PP, which were synthesized using different catalysts, was also studied. Further, the effect of substrate nucleation on fractionated crystallization of ZN-PP droplets was investigated in the presence of different amorphous substrates. Crystallization of ZN-PP droplets in polycarbonate (PC) and polymethyl methacrylate (PMMA) matrices was carried out and compared with crystallization of droplets in PS matrix.

EXPERIMENTAL

Materials and processing

ZN-PP was received from The Dow Chemical Company. ZN-PP used was ZN5D98 with a bulk density 0.900 g/cm^3 (ASTM D792) and melt flow index of 3.4 g/10 min (ASTM D 1238). Dow Styron 685D polystyrene (PS) with bulk density 1.040 g/cm^3 (ASTM D792) and melt flow index of 1.5 g/10 min (ASTM D1238) was used for multilayer extrusion. Multilayered films of ZN-PP/PS were produced as described previously.[12] The films composed of 257 alternating layers of ZN-PP and PS, with 10/90 (vol/vol) composition. ZN-PP layer thickness varied from 12 to 200 nm by changing the total film thickness. A sacrificial PS skin layer was added before the film exited from the die creating a final film of PS/[PP/PS]PS with 30/[4/36]/30 composition.

To investigate the effect of additives, an additive-free polypropylene (cPP) was obtained from The Dow Chemical Company. cPP was synthesized using a Ziegler-Natta catalyst without any additives or stabilizers. Physical properties of the cPP were maintained similar to ZN5D98. Antioxidants Irganox 1010, a hindered phenol (Irganox) and Irgafos 168 an aryl phosphate (Irgafos) were obtained from Ciba Specialty Chemical, now part of BASF. Zinc stearate (ZnS) was obtained from Sigma-Aldrich (St. Louis, MO). The details of the additives are listed in Table I.

Prior to coextrusion, cPP and PS were blended with the additives in a Haake Rheomix 600 twin screw extruder with barrel temperature set at 230°C to produce 2.0% masterbatches of Irganox, Irgafos, and ZnS. Additives were also added to the PS in order to avoid diffusion out of the PP layers during coextrusion. Totally, 257 layered films of cPP/PS with 0.001, 0.1, and 1.0% additive concentrations were coextruded with 10/90 (vol/vol) composition. cPP layer thicknesses were maintained similar to ZN-PP layer thicknesses. A sacrificial PS skin layer was also added.

To study the effect of different catalyst residues, three grades of polypropylene (PP) were investigated. Two homopolymers developed by The Dow Chemical Company were, a commercial grade ZN-PP and a developmental PP prepared with a post-metallocence

TABLE II
Grades of PP Synthesized Using Different Catalysts

Polymer	Designation	$M_w \times 10^{-3}$	X_c[a] (%)	T_m (°C)
Dow Ziegler-Natta PP	ZN-PP	312	43	163
ExxonMobil Metallocene PP	M-PP	≈100	43	152
Dow Developmental PP	D-PP	342	43	147

[a] Calculated from heat of fusion of α-phase PP, $\Delta H = -210$ J/g.
M_w = weight average molecular weight of PP.

catalyst (D-PP). Another grade of PP synthesized by metallocene based catalyst (M-PP) was acquired from ExxonMobil. Details of the molecular weights and molecular weight distributions are shown in Table II. Melting temperatures for M-PP and D-PP were 152 and 147°C respectively, which were lower than ZN-PP melting temperature for 163°C. ZN-PP and D-PP were coextruded with Dow Styron 685D polystyrene (PS) at processing temperature of 255°C. M-PP was extruded with rheologically compatible Dow Styron 615APR polystyrene (MFI = 14.0 g/10 min, 200°C/5.0 kg, ASTM D1238).

The effect of confining substrate on fractionated crystallization of ZN-PP droplets was investigated in PMMA and PC matrices. A total of 257 layered films of ZN-PP/PMMA and ZN-PP/PC with 10/90 (vol/vol) composition were produced. Multilayered films were made by extruding ZN-PP with PC (Calibre 200-15, MFI = 15.0 g/10 min, 300°C/1.2 kg, ASTM D1238) and PMMA (Plexiglass V826, MFI = 1.6 g/10 min, 230°C/3.8 kg, ASTM D1238). ZN-PP/PMMA and ZN-PP/PC films with 10/90 composition with the target PP layer thicknesses 12, 20, 40, and 200 nm were produced. The resulting fractionated crystallization in PMMA and PC was compared with ZN-PP droplets crystallization in PS matrix.

Thermal break up of nanolayers

Perkin Elmer DSC-7 was used in order to breakup the PP layers into droplets. DSC was calibrated for temperature using tin and indium. Extruded film assemblies were heated at 230°C for 3 min, which was well above the T_g of confining substrate and T_m of PP. Control films of PS, PC, and PMMA were also subjected to the same thermal treatment for characterization. Cooling thermograms after the layer breakup were recorded at a rate of 10°C/min. DSC thermograms were normalized for weight. PS, PC, or PMMA contribution was subtracted from the corresponding composite thermograms. Enthalpy and crystallinity values were calculated by normalizing the weight to 100% PP. The heats of fusion for the PP were taken as −210 J/g for α-form and −164 J/g for the meophase.[14,15]

Layer structure

Multilayered films were embedded in epoxy and microtomed at −60°C perpendicular to the plane of the film using a cryo-ultramicrotome (MT6000-XL from RMC). Cross sections of the multilayered films were scanned using the Nanoscope IIIa atomic force microscope (AFM) from Veeco Instruments under the tapping mode at ambient conditions.

Size distribution and morphology of droplets

In PP/PS systems, PP droplets were isolated by selectively dissolving the PS matrix using toluene. A thin film of suspended PP droplets was cast on a glass slide for observation under an optical microscope (OM) and AFM to obtain particle size distribution and morphology images. OM was used in transmission mode with an Olympus (Lake Success, NY) BH-2 microscope. The images of the submicron size PP droplets were scanned using Nanoscope V AFM from Veeco Instruments under the tapping mode at ambient conditions. In the case of ZN-PP/PC system, chloroform was used to selectively dissolve PC. ZN-PP droplets were analyzed using OM and AFM as described here.

X-ray scattering

Wide angle X-ray scattering (WAXS) patterns of PP droplets dispersed in the PS or PC matrix were

TABLE III
Crystallization Enthalpies of cPP Droplets Produced from 200-nm Layers

Irganox concentration (wt %)	Crystallization Exotherms T_{c1}, T_{c2}, T_{c3} (°C)	ΔH_1 at T_{c1} (J/g)	ΔH_2 at T_{c2} (J/g)	ΔH_3 at T_{c2} (J/g)	ΔH_3 at T_{c3} (J/g)	ΔH (J/g)	Crystallinity, X_c[a] (%)
ZN-PP*	66, 88, 103	−3.9	−33.0	−46.2	–	−83.1	40
0.001	66, 91, 106	−7.2	−27.1	−47.6	–	−82.0	39
0.1	66, 90, 107	−3.7	−15.6	−56.9	–	−76.2	36
1.0	66, 90, 107, 112	–	−0.6	−4.0	−74.0	−78.6	37

[a] Calculated from heat of fusion of α-phase PP, $\Delta H_f = -210$ J/g.
* ZN-PP contained 0.001% of Irganox.
ΔH_1, ΔH_2, ΔH_3 are the enthalpy of crystallization at T_{c1}, T_{c2}, T_{c3}.
$\Delta H = \Delta H_1 + \Delta H_2 + \Delta H_3$.

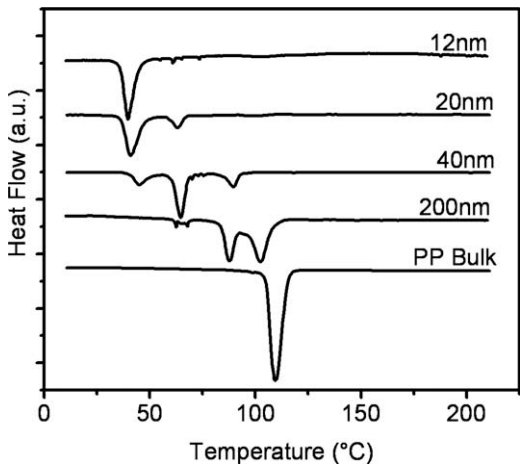

Figure 1 Cooling thermograms of ZN-PP droplets formed by thermal break up of nanolayers at 230°C. PS contribution was subtracted from the composite ZN-PP/PS thermograms. Thermograms were obtained at 10°C/min. The starting layer thicknesses are as labeled.

obtained at ambient temperature in the transmission mode in a Rigaku diffractometer. A sealed-tube source of CuKα radiation operated at 40 kV and 40 mA was used. WAXS patterns of PS and PC control films subjected to same thermal history were also recorded for further analysis.

RESULTS AND DISCUSSION

Fractionated crystallization of ZN-PP droplets in PS

Multilayered films of ZN-PP and PS were successfully produced using layer multiplying coextrusion process. Cross sections of the coextruded films with 12-, 20-, 40-, and 200-nm ZN-PP layers showed good layer uniformity and integrity as reported previously.[12] Interfacial-driven thermal breakup of the multilayered films resulted in the formation of the ZN-PP droplets dispersed in the PS matrix. Solidified ZN-PP droplets showed that the droplet size distribution was dependent on the starting layer thickness. When the starting layer thickness was 12 nm, most of the droplets were produced in a submicron size range of 100–1000 nm. As the layer thickness changed to 20 nm, bimodal distribution of droplets was observed. With further increase in the layer thickness to 40 and 200 nm, all the droplets were formed in 8–10 μm range.

Cooling thermograms of ZN-PP droplets showed four distinct crystallization exotherms ~ at 40, 64, 90, and 103°C, Figure 1.[13] It was observed that the initial layer thickness significantly affected the fraction of ZN-PP droplets crystallized at each temperature. The submicron size droplets devoid of any bulk nuclei were produced from 12-nm layers. The cooling of ZN-PP droplets from 12-nm layers from the melt resulted in the exclusive homogeneous nucleation at 40°C. As the droplet size increased, the number of the droplets that contained different types of heterogeneous nuclei also increased leading to heterogeneous nucleation. When the starting layer thickness was 20 nm, the crystallization of droplets showed an exotherm at 64°C, which was designated as a low order α-phase peak. Decreased intensity of 40°C exotherm was indicative of reduced fraction of homogeneously nucleated droplets. Other high temperature crystallization exotherms at 90 and 103°C were mainly observed in the droplets produced from 40 nm and thicker layers. The presence of higher temperature crystallization exotherms was attributed to activation of the heterogeneous nuclei contained in the ZN-PP droplets. High temperature crystallization peaks produced monoclinic α-crystal form as confirmed by WAXS.

Additives in ZN-PP

Various heterogeneities present in ZN-PP were identified to investigate the origins of 64, 90, and 103°C crystallization exotherms. Additives that can act as possible nuclei are summarized in Table I. Irganox and Irgafos were present up to 1000-ppm concentration. ZN-PP also contained talc, which acted as a neutralizer. It also contained Ziegler-Natta catalyst residues, which were used to synthesize the polymer. Because the fractionated crystallization of the ZN-PP droplets was carried out in PS matrix, it was necessary to identify the additives present in PS. Diffusion of additives from PS was also speculated to affect the fractionated crystallization. ZnS was identified as a mold release agent present in PS.

In this work, the additives (except talc) were selectively added to cPP/PS multilayered films at higher concentrations during coextrusion process. It should be noted that each additive was added separately to cPP/PS films. Three sets of multilayered film samples containing Irganox, Irgafos and ZnS were obtained. It is suggested that the high concentration of additives in layered films increase the number of the droplets containing these additive nuclei. By comparing the crystallization enthalpies at various concentrations, it is possible to assign the origin of crystallization peak to a specific additive.

Effect of additives on crystallization of cPP droplets

Thermal break up of multilayered films containing additives resulted into the dispersion of cPP droplets in a PS matrix. The resulting droplet size distribution was not affected in the presence of the additives in the concentration range studied. Totally, 12-nm layers revealed submicron size cPP droplets. Thicker

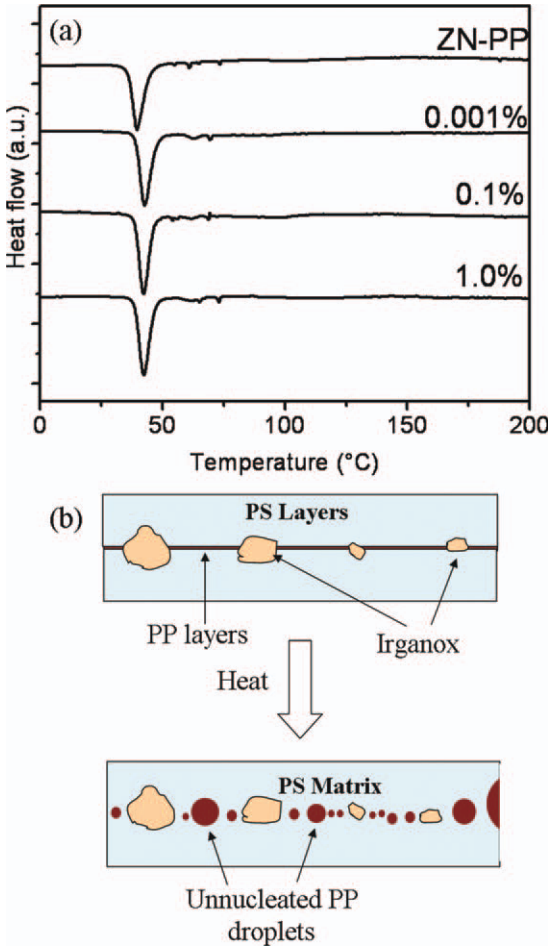

Figure 2 (a) Cooling thermograms of cPP and ZN-PP droplets obtained from 12 nm layers after thermal break up at 230°C. PS contribution was subtracted from the composite PP/PS thermograms. The cooling thermograms were obtained at 10°C/min. The concentration of Irganox used in cPP layers is as labeled. (b) Schematic of thermal break up of cPP layers containing Irganox particles. Irganox particles were excluded from the droplets. [Color figure can be viewed in the online issue, which is available at wileyonlinelibrary.com.]

layers, 40 and 200 nm, resulted in 8–10 μm size cPP droplets, which was also similar to ZN-PP droplet size distribution. (Results not shown here).

Effect of Irganox

Evaluation of crystallization behavior of cPP droplets produced from 12-, 40-, and 200-nm layers at different Irganox concentrations is carried out. The detailed results are shown in Figures 2, 3, and 4.

Effect of Irganox on the crystallization of cPP droplets from 12-nm layers is shown in Figure 2(a). Crystallization of droplets did not show any significant changes when compared with ZN-PP crystallization thermogram. At different Irganox concentrations, cPP droplets were crystallized by homogeneous nucleation at 43°C. It is suggested that Irganox particles were excluded during the break up process, due to the possibility of Irganox particles' size bigger than the layer thickness of 12 nm. Previously, it was established that Irganox is soluble in PP at the processing temperature.[16] However, during cooling from the melt, Irganox must have precipitated out to form larger agglomerates. Resulting agglomerates were excluded from the droplets during thermal break up of 12-nm layers. Schematic of layer break-up in 12 nm layers is proposed as shown in Figure 2(b).

As the starting layer thickness increased to 40 nm, the crystallization of resulting droplets showed three exotherms at 44, 64, and 90°C. Crystallization thermograms of cPP droplets from 40-nm layers are shown in Figure 3. The crystallization peak positions were not affected in the presence of Irganox, when compared with crystallization of ZN-PP droplets. The intensity of 90°C crystallization exotherm was affected slightly with increasing concentration of Irganox. At 1.0% Irganox concentration, very weak exotherm at 110°C was observed. It must be noted that the nuclei were usually be accommodated in the droplets when the size was smaller than the starting layer thickness. The larger nuclei were excluded from the droplets during the layer break up process, which was similar to thermal break up of 12-nm layers as shown in Figure 2(b). Larger agglomerates acted as defects during the thermal break up of layers. Exclusion of nucleating agents in micron size range from the droplets during layer break up process is previously shown by Jin et al.[17]

Further increase in the cPP layer thickness to 200 nm resulted into the formation of 8–10 μm size droplets. Fractioned crystallization of the resulting droplets is shown in Figure 4(a). In this case,

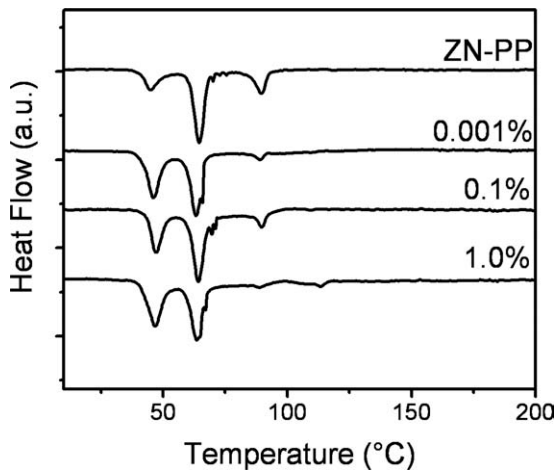

Figure 3 Cooling thermograms of cPP and ZN-PP droplets obtained from 40-nm layers after thermal break up at 230°C. PS contribution was subtracted from the composite PP/PS thermograms. The cooling thermograms were obtained at 10°C/min. Concentration of Irganox used in cPP layers is as labeled.

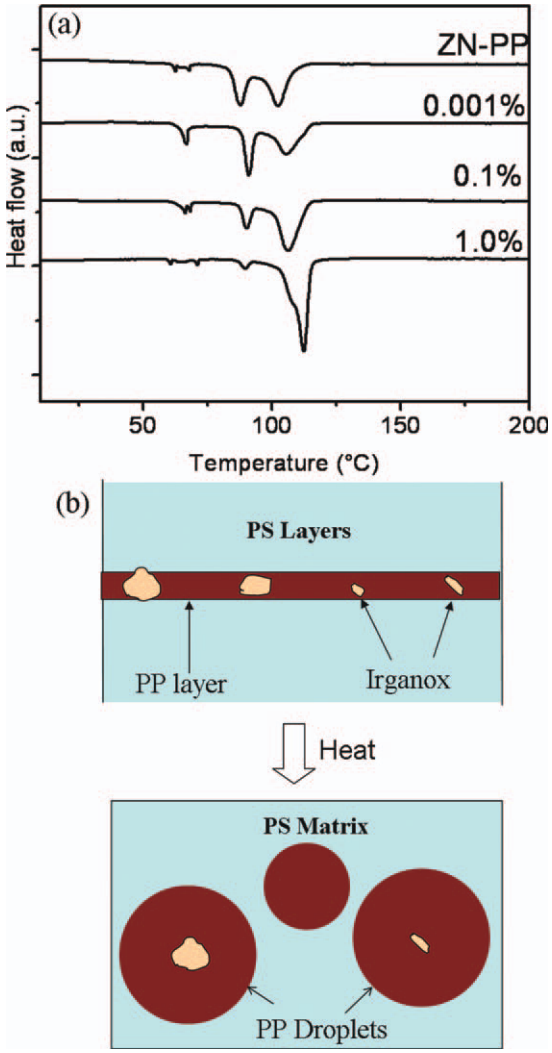

Figure 4 (a) Cooling thermograms of cPP and ZN-PP droplets obtained from 200-nm layers after thermal break up at 230°C. PS contribution was subtracted from the composite PP/PS thermograms. The cooling thermograms were obtained at 10°C/min. Concentration of Irganox used in cPP layers is as labeled. (b) Schematic of thermal break up of cPP layers containing Irganox particles. Irganox particles were encapsulated in the droplets during layer break up process. [Color figure can be viewed in the online issue, which is available at wileyonlinelibrary.com.]

fractionated crystallization of cPP droplets was significantly different than crystallization of ZN-PP droplets. Two main crystallization peaks for ZN-PP droplets were observed at 88 and 103°C, with enthalpies −33.0 and −46. 2 J/g. Cooling thermograms of cPP droplets also revealed two main crystallization peaks. Relative intensities of the two exotherms were affected significantly with increasing Irganox concentration. At very small concentration of 0.001%, two crystallization exotherms at 91 and 105°C with enthalpies −27.1 and −47.6 J/g were observed. The peak positions were affected only slightly when compared with ZN-PP results, which contained same amount of Irganox (0.001 wt %). At higher concentrations of Irganox, intensity of 90°C peak decreased to −15.6 at 0.1 wt % and to −4.0 J/g at 1.0 wt % concentration. It was observed that Irganox crystallize most of the cPP droplets by activating at higher temperature of 107°C. It indeed acted as a nucleating agent at higher concentration. Because the concentration of the Irganox increased the effective nuclei density, the number of droplets containing critical size Irganox nuclei also increased significantly. Crystallization of a large fraction of droplets occurred by heterogeneous nucleation. Significant changes in the crystallization peak position and the enthalpy in crystallization exotherms were indicative of strong effect of Irganox. The nuclei size of Irganox particles was speculated to be smaller than the starting layer thickness, which led to the encapsulation of the nuclei during the layer breakup. The schematic of thermal layer break-up is shown in Figure 4(b). The results of crystallization behavior of droplets from 200-nm layers indicated that the high temperature exotherm in ZN-PP at 103°C resulted from Irganox.

Effect of Irgafos and ZnS

The effect of Irgafos and ZnS on fractionated crystallization of cPP was also investigated. Unlike Irganox, Irgafos and ZnS did not show any significant effect on the crystallization behavior of cPP droplets from various layer thicknesses. (Results for Irgafos and ZnS are not shown.) Based on the observations, it was suggested that Irgafos and ZnS were not responsible for the crystallization of ZN-PP droplets at 64, 90, or 100°C.

Effect of catalyst residues

ZN-PP grade contained traces of Ziegler-Natta catalyst residues. As suggested earlier, the catalyst residues were also potential nuclei for the heterogeneous nucleation of ZN-PP droplets. To investigate the effect of catalysts, fractionated crystallization of different grades of PP was studied in this section. PP is usually synthesized by various catalysts such as Ziegler-Natta, metallocene, and post-metallocene. Three grades of PP produced using different catalysts are listed in Table II. Fractionated crystallization of PP droplets produced from these grades is reported in Figures 5 and 6.

Crystallization of PP droplets from 12-nm layers of ZN-PP and D-PP showed a main crystallization peak at 40 and 37°C, respectively [Fig. 5(a)]. It confirmed that the crystallization of PP droplets occurred in the absence of any heterogeneities. Results showed exclusion of catalyst residues from the PP droplets during break up process. Crystallization enthalpy of −30.6 J/g in M-PP droplets was

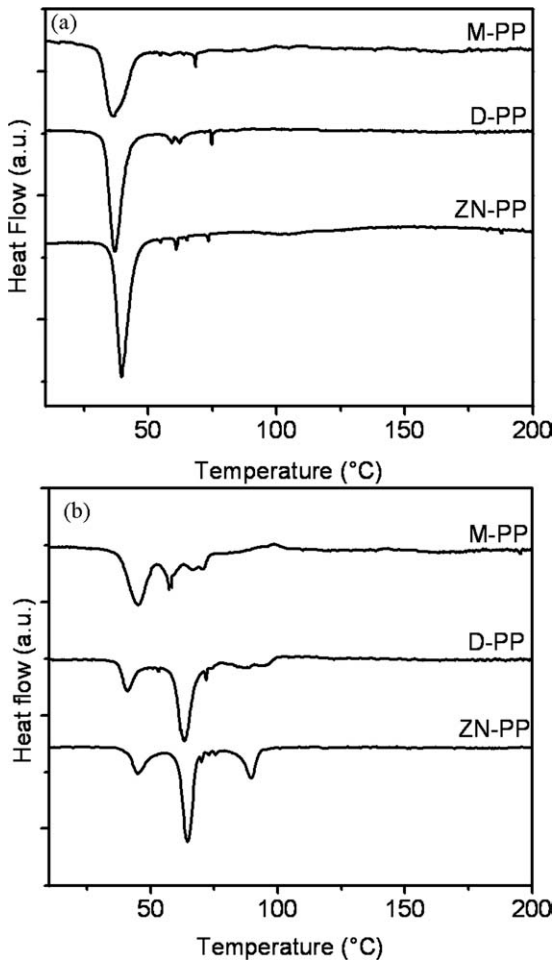

Figure 5 Cooling thermograms of PP droplets obtained from (a) 12-nm layers (b) 40-nm layers. Grades of PP used are as labeled. PS contribution was subtracted from the composite PP/PS thermograms. The cooling thermograms were obtained at 10°C/min.

slightly lower than crystallization enthalpies of −36.0 and −36.2 J/g in D-PP and ZN-PP droplets. It must be noted that the molecular weight of M-PP was significantly lower than molecular weights of ZN-PP and D-PP grades. A smaller and broader homogeneous nucleation peak in M-PP droplets was attributed to low molecular weight.

The crystallization behavior of ZN-PP and D-PP droplets was not significantly different in the droplets from 40-nm layers, Figure 5(b). Three main crystallization peaks at 40, 63, and 90°C were not affected. However, unlike ZN-PP and D-PP, M-PP showed a stronger 40°C and weak 60°C crystallization peaks, suggesting an important role of molecular weight on the fractionated crystallization.

Fractionated crystallization of droplets from thicker layers, 200 nm, is reported in Figure 6(a). Crystallization of ZN-PP droplets showed two main peaks at 103 and 90°C. When a postmetallocene-based D-PP was used, the crystallization was more prominently observed at 103°C, with a weak shoulder at 90°C. In contrast, M-PP showed multiple small crystallization peaks in a temperature range 60–90°C, Figure 6(a). It should be noted that D-PP and ZN-PP have comparable molecular weights (Table II). The results suggest the possibility of nucleation of 90°C crystallization peak in the case of ZN-PP droplets by catalyst residues. It is assumed that the additives and stabilizers present in ZN-PP and D-PP grades were not different in two polymers.

1D-WAXS patterns of the droplets from 200-nm layers is shown in Figure 6(b). Although the crystallization exotherms of droplets from 200-nm layers showed significantly different results, the crystal structure of PP in the droplets was not affected. Different crystal reflections for α(110), α(040), α(111), and α(041) crystal planes were observed in all the samples confirming the presence of monoclinic α-phase in the droplets.

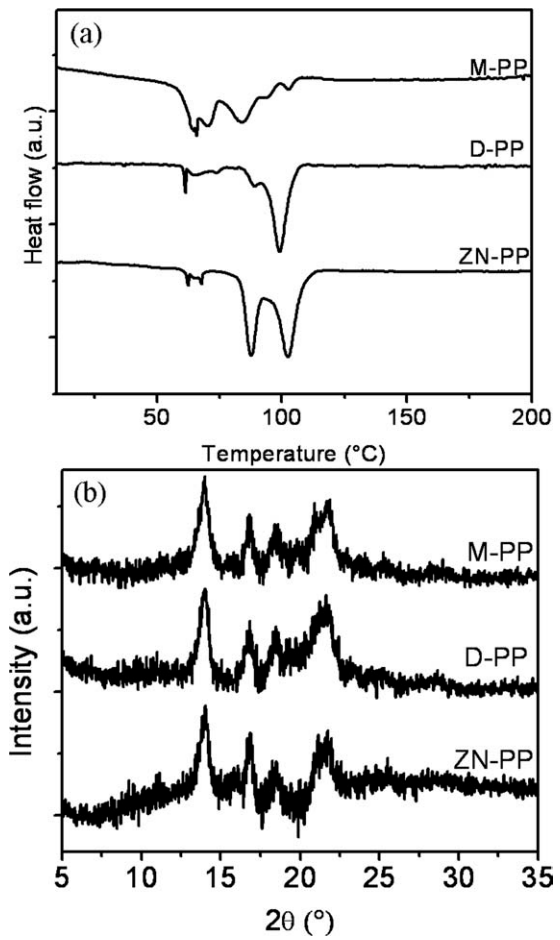

Figure 6 (a) Cooling thermograms of PP droplets obtained from 200-nm layers. Grades of PP used are as labeled. PS contribution was subtracted from the composite PP/PS thermograms. The cooling thermograms were obtained at 10°C/min. (b) 1D-WAXS patterns of PP droplets from 200-nm layers, obtained after subtraction of PS contribution.

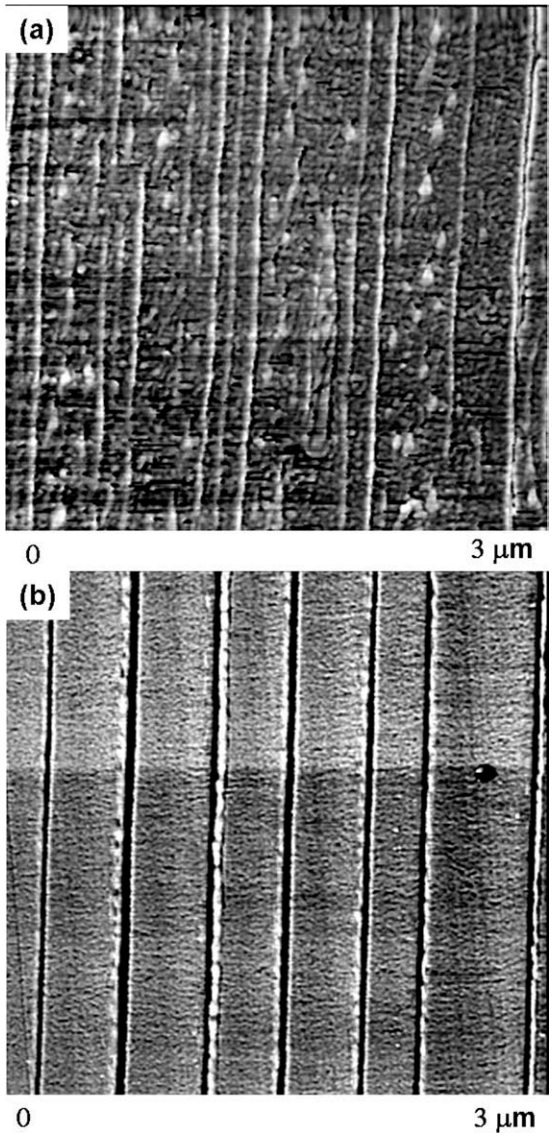

Figure 7 AFM phase images of the cross-sections of coextruded ZN-PP/PC films with (a) 12-nm ZNPP layers, (b) 40-nm ZN-PP layers.

Effect of confining substrates on crystallization of ZN-PP droplets

In addition to different heterogeneous nuclei present in the bulk, it was suggested that the nuclei from the substrate or the substrate itself can be responsible for heterogeneous nucleation of PP droplets. Crystallization of ZN-PP droplets under the confinement amorphous polymers was investigated. ZN-PP was extruded against three different amorphous polymers–PS, PMMA, and PC. Effect of PS matrix on the crystallization of ZN-PP droplets is reported earlier in Figure 1. Crystallization thermograms of ZN-PP droplets in PMMA matrix were not different from crystallization of droplets in PS matrix (Results are not shown here). Unlike PS and PMMA, PC matrix impacted the crystallization behavior of the ZN-PP droplets. Detailed analysis of ZN-PP/PC system is reported here.

Effect of PC substrate

Prior to thermal break up of ZN-PP/PC films, the layered structure was investigated for integrity and uniformity by AFM. Examples of cross-sections of layered films with ZN-PP nominal layer thickness of 12 and 40 nm are shown in Figure 7. AFM images showed continuous ZN-PP and PC layers with desired layer thicknesses. Layering periodicity in a 15-μm film matched with the combined ZN-PP and PC layer thicknesses as it was difficult to measure

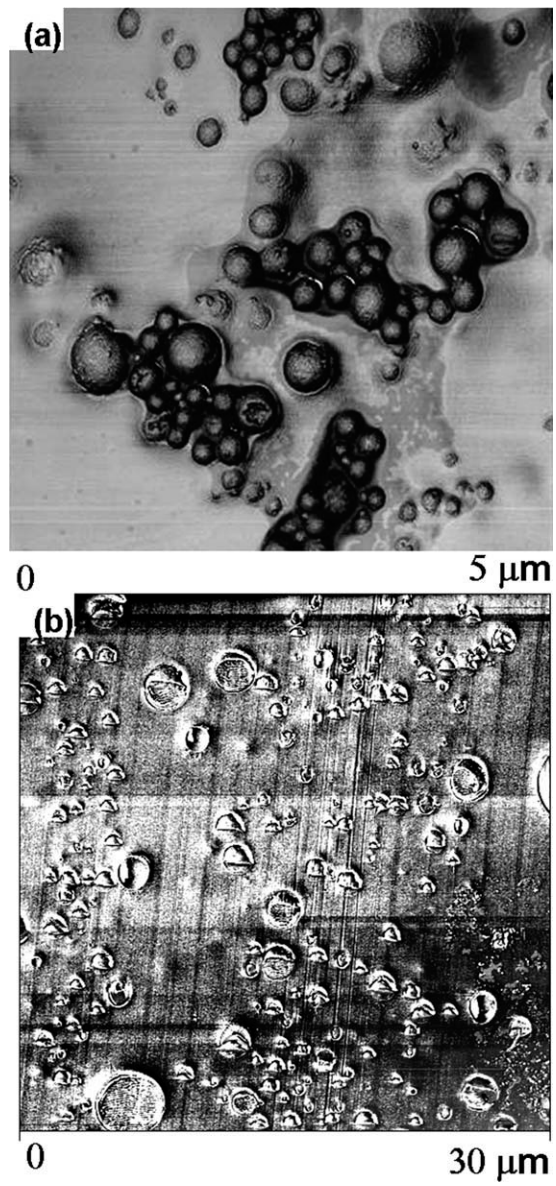

Figure 8 AFM images of ZN-PP droplets produced from (a) 12-nm layers (b) 40-nm layers. The droplets were produced by thermal breakup of ZN-PP/PC multilayered films at 230°C.

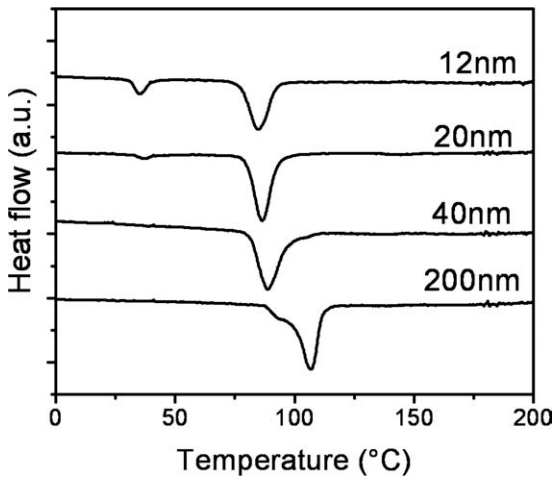

Figure 9 Cooling thermograms of ZN-PP droplets formed by thermal break up of ZN-PP/PC films at 230°C. PC contribution was subtracted from the composite thermograms. Thermograms were obtained at 10°C/min. The starting layer thicknesses are as labeled.

the individual layer thickness in 12-nm ZN-PP layer films due to a tendency of layer pullout during microtoming. Continuous ZN-PP layer with 40 nm thickness were observed [Fig. 7(b)].

Dispersions of the ZN-PP droplets were obtained in a PC matrix by heating the films to 230°C. For imaging solidified submicron size ZN-PP droplets from 12-nm layers, PC matrix was selectively dissolved in chloroform and a suspension of ZN-PP droplets was cast on a glass slide for AFM scanning. A high resolution image of the ZN-PP droplets produced from the 12-nm layers showed the presence of submicron size droplets in a 100–800 nm range [Fig. 8(a)]. ZN-PP droplet size was not affected in the presence PC matrix, as the results were comparable with the droplets produced after thermal break up in a PS matrix.[12] For the droplets from 40-nm layers, the cross section of the stacks of the films was imaged using AFM after microtoming. PP droplets in a size range up to 6–8 μm were observed [Fig. 8(b)].

Crystallization thermograms of ZN-PP droplets in PC matrix are shown in Figure 9. Three crystallization exotherms were observed at 107, 85, and 40°C. Initial layer thickness strongly impacted the relative intensities of the crystallization peaks. Corresponding crystallization enthalpies are tabulated in Table IV.

Droplets from 12 nm showed a main crystallization peak at 85°C and a small peak at 37°C in submicron size droplets. In the presence of PC, ~ 80% PP nucleated heterogeneously at 85°C and remaining fraction nucleated homogenously at 37°C. Previously, droplets from 12-nm layers were crystallized at 43°C by homogeneous nucleation into mesophase in a PS matrix (Fig. 1). The mesophase formation was also confirmed by the presence of broad peaks at 15 and 21° in 1D-WAXS patterns.[18] Crystallization of ZN-PP droplets at higher temperature suggested that PC indeed acted as a nucleating agent for ZN-PP droplets. The aromatic backbone of the PC chain can be a nucleating site for ZN-PP nucleation. Alternatively, the possibility of nuclei migration from the PC matrix into the droplets can not be ruled out. It is concluded that the heterogeneous nuclei or the substrate nucleation was activated at 85°C. Previously, the crystallization of PP droplets at 85°C was reported in PP/PC blends with 20% PP.[19] It is important to note that the substrate nucleation from PC is activated at 85°C, which is not possible to observe in bulk crystallization of ZN-PP as it crystallizes at 110°C.

As the starting layer thickness increased to 20 and 40 nm, most of the droplets were crystallized heterogeneously at 85°C. Droplets from 40-nm layers showed a principle crystallization exotherm at 85°C. This peak was specific to the ZN-PP droplets in PC matrix. Absence of 60°C peak was also unique to this system, which was previously reported in droplets crystallizing in a PS matrix. Because all the droplets were crystallized at 85°C, the nuclei responsible for 60°C crystallization exotherm were not activated. The droplets created from 200-nm layers showed main crystallization peak at 107°C, which

TABLE IV
Crystallization Enthalpies of ZN-PP Droplets Produced from ZN-PP/PC Multilayered Films

Layer thickness (nm)	Temperature (°C)	ΔH_s (J/g)	Temperature (°C)	$\Delta H_{\alpha 1}$ (J/g)	Temperature (°C)	$\Delta H_{\alpha 2}$ (J/g)	ΔH_α Total (J/g)	X_s (%)	X_α (%)	X_t (%)
12	36	−8.3	85	−43.3	–	–	−51.6	5	21	26
20	37	−2.6	86	−53.4	–	–	−56.0	2	25	27
40	–	–	89	−61.7	–	–	−61.7	0	29	29
200	–	–	92	–	107	−63.1	−63.1	0	30	30
ZN-PP	–	–	–	–	110	0	−89.0	0	43	43

X_s calculated from heat of fusion of mesophase PP, $\Delta H_s = -164$ J/g.
X_α calculated from heat of fusion of α-phase PP, $\Delta H_f = -210$ J/g.
$\Delta H = \Delta H_1 + \Delta H_2 + \Delta H_3$.
$X_t = X_s + X_\alpha$.

was close to the bulk crystallization exotherm at 110°C. In addition to this peak, a small shoulder at 92°C was observed, which was most likely due to the bulk nuclei reported in the earlier sections.

WAXS patterns of the ZN-PP droplets, obtained after subtraction of PC contribution are shown in Figure 10. The droplets from 20-, 40-, and 200-nm layers also showed α-phase crystal reflections for α(110), α(040), α(111), and α(041) crystal planes. In 12-nm layers, WAXS patterns of the particle dispersions showed strong α-phase reflections confirming the heterogeneous nucleation in submicron size droplets. Previously, mesophase formation was reported in ZN-PP droplets crystallized in a PS matrix. Formation of α-phase in submicron size droplets was unique to the droplets crystallized in a PC matrix.

Morphology of submicron size ZN-PP Droplets in PC matrix

It was interesting to note that the submicron size droplets (100–1000 nm) were nucleated heterogeneously. Further investigation of the heterogeneously nucleated submicron size ZN-PP droplets from 12-nm layers was preformed. Morphological features of the droplets are shown in Figure 11. ZN-PP droplets showed two types of morphologies. Figure 11(a) shows cross-hatched lamellar morphology confirming the presence of α-phase. A few droplets with granular morphology were also observed as shown in Figure 11(b). AFM confirmed the two different crystal forms of ZN-PP droplets observed in DSC thermograms (Fig. 9). The cross-hatched morphology was assigned to the crystallization of droplets at 85°C, while the granular morphology was attributed to homogeneous nucleation at 37°C.

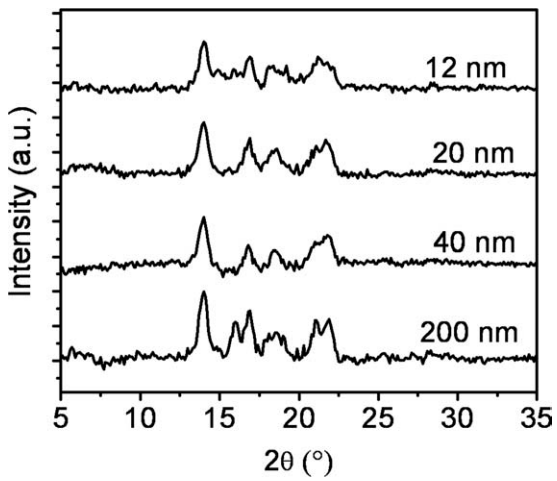

Figure 10 1D WAXS patterns of the ZN-PP droplets produced from thermal break up of nanolayers. Results were obtained after subtraction of the PC contribution.

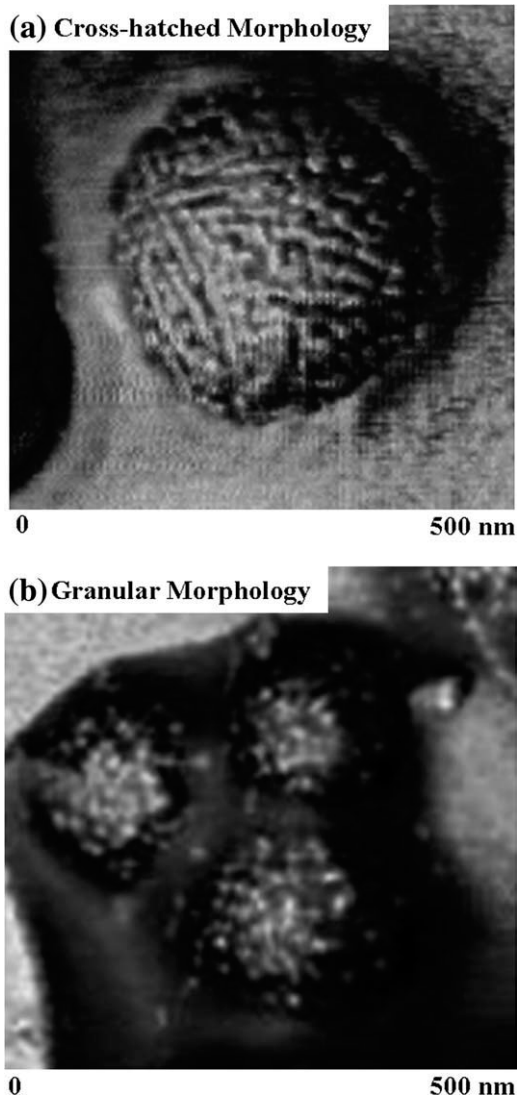

Figure 11 AFM images of PP droplets from 12-nm layers with (a) cross-hatched alpha phase lamellar morphology, and (b) granular mesophase morphology.

CONCLUSIONS

Fractionated crystallization of Ziegler-Natta polypropylene (ZN-PP) droplets produced by thermal break up of multilayered films was investigated. Crystallization of ZN-PP droplets showed four distinct exotherms at 40, 64, 90, and 103°C. Relative intensities of the exotherms were affected by the number of droplets and droplet size distributions, which were strongly dependent on the starting layer thickness. The goal of this paper was to investigate the origins of the 64, 90, and 103°C crystallization exotherms, which were attributed to different heterogeneities present in ZN-PP. The heterogeneities were separated and activated during the fractionated crystallization process. The lowest crystallization peak at 40°C was assigned to homogeneous nucleation. Various nucleating heterogeneities that can be

responsible for crystallization of ZN-PP droplets were investigated in this paper by analyzing the nucleation of PP droplets in the presence of different additives, catalyst residues, and substrates.

Various additives present in the ZN-PP and PS were identified as possible nuclei responsible for various crystallization exotherms. Two additives investigated in this study were Irganox and Irgafos, which were present in bulk ZN-PP as antioxidants. Another additive, Zinc Stearate (ZnS), was present in PS. It is suggested that ZnS migrated to PP droplets from PS layers during the coextrusion process, and affected the fractionated crystallization of ZN-PP droplets. The additives were selectively added to multilayered films of additive-free ZN-PP (cPP) and PS. Crystallization of cPP droplets produced from 12, 20, and 40 nm was not affected when Irganox was present in the layers. However, the droplets from 200-nm layers showed significant effect of Irganox concentration on the crystallization enthalpy of the 103°C peak. It was concluded that Irganox was responsible for crystallization of droplets at 103°C in ZN-PP droplets. In contrast, Irgafos and ZnS did not show any effect on fractionated crystallization of cPP.

To investigate the effect of catalyst residues, fractionated crystallization of three grades of PP were examined. The PPs were ZN-PP, a developmental PP (synthesized by post-metallocene catalysts) and a metallocene PP (synthesized by metallocene catalysts). Crystallization of PP droplets from 12-nm layers showed homogeneous nucleation in all three polymers. Major differences in the crystallization of droplets from 200-nm layers were observed. Crystallization of ZN-PP droplets was mainly observed at 90 and 103°C, while D-PP showed crystallization peak at 100°C. M-PP droplets exhibited multiple crystallization exotherms in temperature range of 60–90°C, which were attributed to its lower molecular weight than ZN-PP and D-PP. It is suggested that the origin of the 90°C peak in ZN-PP was most likely due to catalyst residues.

The effect of confining matrix on fractionated crystallization of ZN-PP droplets was investigated to examine the possibility of substrate nucleation or nuclei migration from the amorphous matrix. When the confining substrate was changed from polystyrene (PS) to polymethyl methacrylate (PMMA), the crystallization of ZN-PP droplets was unaffected. In the case of polycarbonate (PC) substrate, the fractionated crystallization of ZN-PP droplets occurred at 85°C in the droplets produced from all layer thicknesses studied. This nucleation behavior was unique to the ZN-PP/PC system. The crystallization peak at 85°C suggested that the PC substrate heterogeneously nucleated the ZN-PP droplets. Heterogeneous nucleation was confirmed by the presence of cross-hatched lamellar morphology and crystal reflections of the α-phase.

We successfully identified the origin of the 103 and 90°C peaks in fractionated crystallization of ZN-PP droplets. It was also found that the molecular weight of PP and the confining substrates play an important role in controlling the fractionated crystallization of PP.

References

1. Ghijsels, A.; Groesbeek, N.; Yip, C. W. Polymer 1982, 23, 1913.
2. Morales, R. A.; Arnal, M. L.; Muller, A. J Polym Bull 1995, 35, 379.
3. Woo, E.; Hoo, J.; Jeong, Y.G.; Shin, K. Phys Rev Lett 2007, 98, 136103.
4. Arnal, M. L.; Muller, A. J.; Maiti, P.; Hikosaka, M. Macromol Chem Phys 2000, 201, 2493.
5. Ghijsels, A.; Groesbeek, N.; Yip, C. W. Polymer 1982, 23, 1913.
6. Castillo, R. V.; Arnal, M. L.; Muller, A. J.; Hamley, I. W.; Castelletto, V.; Schmalz, H.; Abetz. Macromolecules 2008, 41, 879.
7. Loo, Y. L.; Register, R. A. Phys Rev Lett 2000, 84, 4120.
8. Loo, Y. L.; Register, R. A.; Ryan, A. J.; Jee, D. T. Macromolecules 2001, 34, 8968.
9. Massa, M. V.; Dalnoki-Veress, K. Phys Rev Lett 2004, 92, 255509.
10. Koutsky, J. A.; Walton, A. G.; Baer, E. J Appl Phys 1967, 38, 1832.
11. Bernal-Lara, T. E.; Liu, R. Y. F.; Hiltner, A.; Baer, E. Polymer 2005, 46, 3043.
12. Jin, Y.; Hiltner, A.; Baer E. J Polym Sci Part B: Polym Phys 2007, 45, 1138.
13. Langhe, D. S.; Keum, J. K.; Hiltner, A.; Baer E. J Polym Sci Part B: Polym Phys 2011, 49, 159.
14. Jin, Y.; Hiltner, A.; Baer, E.; Masirek, R.; Piorkowska, E.; Galeski, A. J Polym Sci Part B Polym Phys 2006, 44, 1795.
15. Bu, H.-S.; Cheng, S. Z. D.; Wunderlich, B. Makromol Chem Rapid Commun 1988, 9, 75.
16. Billingham, N. C.; Clavert, P. D.; Okopi, I. W.; Uzuner, A. Polym Degrad Stabil 1991, 31, 23.
17. Jin, Y.; Hiltner, A.; Baer E. J Appl Poly Sci 2007, 105, 3260.
18. Langhe, D. S.; Hiltner, A.; Baer, E. J Polym Sci Part B: Polym Phys 2011, 49, 1672.
19. Chun, Y. S.; Jung, H. C.; Han, M. S.; Kim, W. N. Polym Engg Sci 1999, 39, 2304.